BioMetals (2006) 19:127–142
DOI 10.1007/s10534-005-5420-0

Characterization of TonB interactions with the FepA cork domain and FecA N-terminal signaling domain

R. Sean Peacock, Valery V. Andrushchenko, A. Ross Demcoe, Matt Gehmlich, Lily Sia Lu, Alicia Garcia Herrero & Hans J. Vogel*
*Structural Biology Research Group, Department of Biological Sciences, University of Calgary, Calgary, Alberta, Canada, T2N 1N4; *Author for correspondence (Tel: +1-403-220-6006; Fax: +1-403-289-9311; E-mail: vogel@ucalgary.ca)*

Received 21 November 2005; accepted 23 November 2005

Key words: fourier transfrom infrared spectroscopy, Gram-negative bacteria, iron transport, nuclear magnetic resonance, TonB

Abstract

The mechanism of TonB dependent siderophore uptake through outer membrane transporters in Gram-negative bacteria is poorly understood. In an effort to expand our knowledge of the interaction between TonB and the outer membrane transporters, we have cloned and expressed the FepA cork domain (11–154) from *Salmonella typhimurium* and characterized its interaction with the periplasmic C-terminal domain of TonB (103–239) by isotope assisted FTIR and NMR spectroscopy. For comparison we also performed similar experiments using the FecA N-terminal domain (1–96) from *Escherichia coli* which includes the conserved TonB box. The FepA cork domain was completely unfolded in solution, as observed for the *E. coli* cork domain previously [Usher *et al.* (2001) *Proc Natl Acad Sci USA* **98**, 10676–10681]. The FepA cork domain was found to bind to TonB, eliciting essentially the same chemical shift changes in TonB C-terminal domain as was observed in the presence of TonB box peptides. The FecA construct did not cause this same structural change in TonB. The binding of the FepA cork domain to TonB-CTD was found to decrease the amount of ordered secondary structure in TonB-CTD. It is likely that the FecA N-terminal domain interferes with TonB-CTD binding to the TonB box. Binding of the FepA cork domain induces a loss of secondary structure in TonB, possibly exposing TonB surface area for additional intermolecular interactions such as potential homodimerization or additional interactions with the barrel of the outer membrane transporter.

Introduction

Gram-negative bacteria are constantly struggling to acquire the iron they need for such diverse biological functions as electron transport and DNA synthesis (Ratledge & Dover 2000), and consequently they have developed creative ways to scavenge it. One of the most common ways in which bacteria achieve this is through the use of iron chelating siderophores. The first hurdle they must overcome in the uptake of these siderophores is their passage through the outer membrane. This is accomplished by cognate outer membrane transporters (OMT) which are dependent on the energy input by the inner membrane TonB/ExbB/ExbD protein complex (Figure 1) (recently reviewed in (Postle & Kadner 2003; Braun 2003; Wiener 2005). Although many siderophore outer membrane transporters have been extensively characterized, the actual method of siderophore transport through these receptors remains unclear.

A number of OMT structures have been solved from *Escherichia coli*, including FepA (Buchanan *et al.* 1999), FhuA (Ferguson *et al.* 1998, 2000),

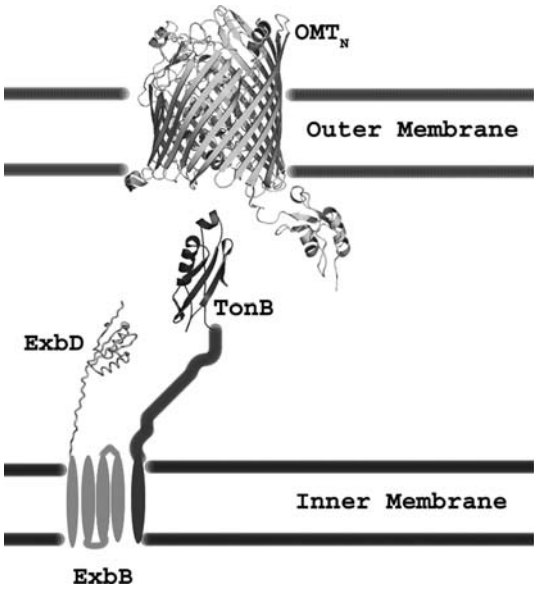

Figure 1. Schematic of TonB dependent iron uptake. Binding of siderophores to the OMT induces a structural change which the cytoplasmic membrane bound protein TonB recognizes and binds to. The ExbB/ExbD proteins transmit the energy of the inner membrane proton gradient through TonB to the OMT, allowing for siderophore transport into the periplasmic space. Some outer membrane receptors have an N-terminal extension (OMT_N) which responds to the presence of the OMT_N's ligand in the extracellular space, resulting in a signaling cascade which induces transcription of an operon encoding for all the proteins involved in that siderophore's transport across the outer and inner membranes.

FecA (Ferguson *et al.* 2002; Yue *et al.* 2003) and BtuB (Kurisu *et al.* 2003) in various ligand free and ligand bound forms. Recently two more structures of outer membrane receptors from *Pseudomonas aeruginosa* have been determined: FpvA (Cobessi *et al.* 2005a) and FptA (Cobessi *et al.* 2005b). In all cases, the structures have been found to be 22 stranded β-barrels with an N-terminal mixed α-helix/β-sheet globular domain, known variously as the plug, the cork or the hatch (hereafter referred to as the cork), blocking the centre of the barrel (Figure 2). Some of these transporters (OMT_N) have N-terminal extensions which extend into the periplasmic space and play a role in the transcriptional regulation of the genes involved in the uptake of transporter's ligand (OMT_N) (Schalk *et al.* 2004; Koebnik 2005; Braun & Mahren 2005). The ferric citrate receptor FecA from *Escherichia coli* is an example of an OMT_N (Figure 3). This N-terminal signaling domain was not resolved in the crystal structure, however an NMR structure of this domain in isolation has been reported (Garcia Herrero & Vogel 2005).

One of the big questions yet to be resolved with regards to TonB dependent transport is what role the cork domain plays in the ligand transport across the outer membrane (Klebba 2003). Does the ligand get passed through the inside of the barrel along a 'transport pathway' contained within the N-terminal cork domain, or is it somehow completely displaced into the periplasm to allow for free passage of the ligand into the periplasm? Also the overall action of the TonB system is still shrouded in mystery (Postle & Kadner 2003). Be that as it may, it is widely believed that TonB binds to the TonB box region of the OMT, which consists of a 5–7 conserved amino acid sequence at the N-terminal end of the cork domain.

Several different studies have attempted to address this issue of cork displacement and stability. Molecular dynamics simulations (Faraldo-Gomez *et al.* 2003) of the FhuA receptor have examined the general stability of the structure as well as the behavior of water molecules within the core of the N-terminal domain. In the course of the simulation, the secondary structure of the cork domain was essentially stable, with the beta sheet region being relatively unchanged, and slightly larger fluctuations in the loops and the first two helices. These authors note that although the average number of hydrogen bonds from the barrel to the cork is large ($\sim$65), other known dissociable protein–protein complexes also sometimes have a similar number of hydrogen bonds. Moreover, the energetic cost of breaking these bonds can be mitigated by forming new hydrogen bonds with bulk water. All of the outer membrane transporter structures contain a narrow solvated channel which is thought to possibly be the conduit along which the siderophore could penetrate through the transporter. During the simulations, it was apparent that substantial rearrangements would be required before ferrichrome could pass through that channel, which were not observed on the timescale of the simulation.

Differential scanning calorimetry studies of FhuA (Bonhivers *et al.* 2001) discerned two distinct melting transitions which the authors attributed to separate cork domain and barrel domain unfolding events, indicating that these two domains can act independently of one another. The

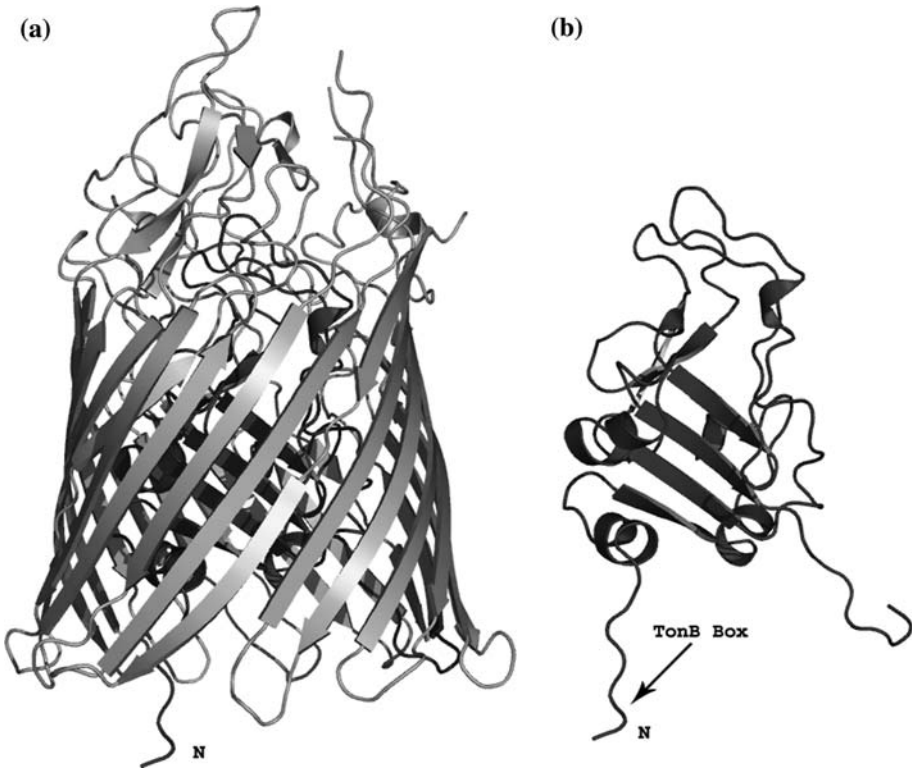

Figure 2. (a) Crystal structure of FepA from *Escherichia coli* (Buchanan *et al.* 1999). (b) The cork domain region of FepA; the same region from *Salmonella typhimurium* was studied in this work. The position of the TonB box region is indicated.

melting transition thought to be primarily due to the cork domain was significantly stabilized by the presence of ferrichrome.

Studies on the reconstitution of the cork domain and barrel domain expressed separately have also been done (Letoffe *et al.* 2005) *in vivo* and *in vitro*. Expression of both the cork domain and the barrel domain resulted in association of the cork domain with the outer membrane fraction presumably due to interactions with the barrel, whereas expression of the cork domain by itself resulted in it being found in the periplasmic space. Binding studies with the hemophore HasA indicated that although the cork domain will not associate with HasA by itself, it does at least associate with the barrel domain in the presence of HasA *in vitro*. However, co-expressing barrel and plug domains did not allow for HasA transport *in vivo*.

To examine more directly the issue of whether outer membrane transporters required ejection of the cork domain from the barrel, an interesting experiment was done where FhuA constructs were made in which disulphide bonds cross-linked the cork domain to the barrel along the proposed siderophore transport channel (Eisenhauer *et al.* 2005). This cross linking did not affect the transport rate of ferricrocin, indicating that it is unlikely that the entire cork is removed intact from the barrel during transport. At the same time though, the disulphide cross links would also interfere with the transport of the siderophore along the solvated channel between the barrel and the cork, arguing against the possibility that this is the path that the siderophores follow through the outer membrane receptor.

Two studies have looked specifically at how these cork domains behave in isolation. In the first, the cork domain of the enterobactin receptor FepA from *Escherichia coli* was studied by Nuclear Magnetic Resonance (NMR) and fluorescence studies (Usher *et al.* 2001). This construct was found to be essentially unfolded in solution. Nonetheless, ferric-enterobactin bound to the cork domain with an affinity of about 5 μM as determined by fluorescence polarization methods,

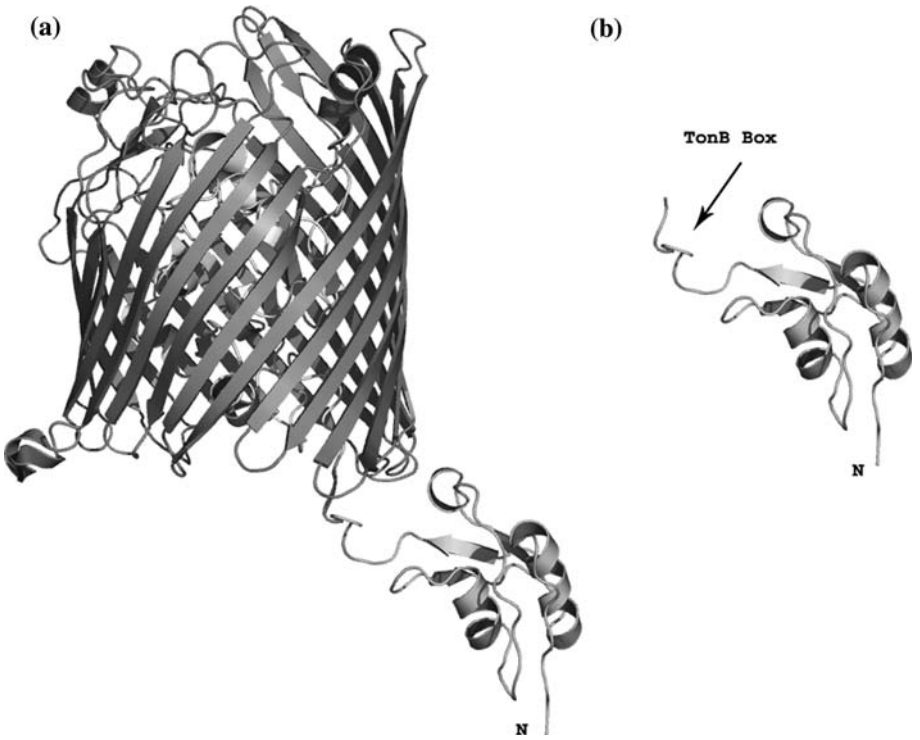

Figure 3. (a) The structure of a representative member of an OMT_N. The crystal structure of ligand free FecA (Ferguson *et al.* 2002) was merged with the solution structure of the N-terminal extension of FecA (1–96) (Garcia Herrero & Vogel 2005) (b) The structure of the isolated N-terminal domain of FecA. This is the same construct which is used in this study. The position of the TonB box region is indicated.

which is about 100 fold reduced in comparison to intact FepA. However, no major shift in the amide resonances of FepA were observed in the presence of gallium-enterobactin, indicating that no major structural changes are occurring that are visible by NMR. In the second study, the *Neisseria meningitides* transferrin receptor (TbpA) cork domain was found to have significant structure in solution by CD spectroscopy, but no indication that it bound it's ligand was observed by either isothermal titration calorimetry or a nitrocellulose binding assay (Oke *et al.* 2004). This would seem to indicate that not all of the cork domains behave similarly in isolation from their barrel.

A detailed analysis of the sequence/structure relationship of the OMTs (Chimento *et al.* 2005) has revealed that most of the highly conserved regions are within areas involved in the interface between the barrel and the cork domains. It was noted that many of the cork domain interactions with the barrel domain are typical of transient protein–protein contacts, characterized by a high proportion of hydrophilic and charged residues. It was also pointed out that relatively small forces are needed to unfold proteins if the force applied is perpendicular to a β-sheet. All these aspects point towards a cork domain structure which is well optimized both for blocking entry in the absence of energy input, yet poised for relatively easy unfolding and ejection given the appropriate application of force.

Like many other groups, we are interested in the interactions between TonB and the outer membrane transporters. Recently we solved the solution structure of TonB-CTD and studied its interactions with small synthetic peptides derived from TonB box regions of OMTs (Peacock *et al.* 2005). The next logical step to take is to study the interactions between TonB-CTD and the intact outer membrane transporters. Because our lab's primary research tool is Nuclear Magnetic Resonance Spectroscopy (NMR), and NMR has particular technical difficulties in looking at large proteins and large protein complexes, we decided

that as a preliminary step we would look at the interactions between TonB-CTD and the cork domains before trying to look at the entire outer membrane transporter. Specifically in this study we have looked at the interaction between TonB-CTD from *E. coli* and the FepA cork domain from *S. typhimurium* as well as the FecA N-terminal extension from *E. coli*. We found that although TonB-CTD can bind to the isolated cork domain of FepA from *Salmonella*, we do not observe any large scale changes in the secondary structure of this cork domain. Similarly to studies of the FepA cork domain from *E. coli*, we were unable to see conformational changes of FepA in the presence of enterobactin by NMR or Fourier transform infrared spectroscopy (FTIR). The chemical shift changes are very similar to the chemical shift changes observed in TonB-CTD in the presence of peptides encompassing the TonB box. In contrast, we were not able to observe these shifts in TonB-CTD in the presence of the FecA N-terminal domain from *E. coli* which encompasses the TonB box. This may indicate that although TonB can bind to isolated TonB box sequences, when considering larger polypeptide portions of the outer membrane receptors, there may be additional binding requirements involving the cork domain.

Materials and methods

Cloning

The nucleotide sequences of the OMTs of FepA, BtuB, FhuA, FhuE, IroN and FoxA from *Salmonella typhimurium* LT2 were retrieved from GenBank, and their cork domains were identified by sequence alignments using ClustalW (Aiyar 2000) and homology modeled using the Swiss-Model capability of SwissPDBViewer (Guex 2001) with the crystal structures of BtuB, FhuA and FepA as templates. Primers were designed so that a 6 histidine extension was present at the C-terminus of the cork domains for purification purposes, as well as a 5′ overhang for cloning purposes in the directional TOPO vector which did not add any residues other than an initiation methionine. The cork domains were cloned beginning from the predicted first amino acid after the signal peptide precursor that is required for export of the OMT across the cytoplasmic membrane. The purified PCR products were cloned into the Invitrogen pENTR/SD/D-TOPO directional TOPO vector, and their sequence was verified by conventional DNA sequencing. These clones were then transferred into the Invitrogen pDEST14 expression vector using the Gateway LR recombination reaction as specified by the manufacturer (Invitrogen). These clones were transformed into BL21(DE3) cells (Invitrogen) and tested for overexpression using 40 ml test cultures. The FepA cork domain (25–175) was by far the best expressed of the proteins. Further purification trials also indicated that it was also the cork domain that was least susceptible to degradation, so all further studies were carried out on this construct.

Purification

All protein was produced either in LB media, or in M9 minimal medium with 0.1% (w/v) $^{15}NH_4Cl$, or ^{13}C Glucose to prepare isotopically enriched protein. Cells were grown to A_{600} ~0.6 at 37 °C and then induced for 20 h at room temperature by adding 0.4 mM isopropyl-β-D-thiogalactopyranoside. Cells were lysed by two passes through a French press at 16 000 psi (1 psi≈6.9 kPa). For the FepA cork domain, clarified cell lysate was purified by nickel affinity chromatography, followed by buffer exchange into 20 mM MES buffer (pH 5.5), and then further purified using a Resource S cation-exchange column (Pharmacia) by running a 0–2 M NaCl gradient. Samples were then buffer-exchanged into 10 mM sodium phosphate (pH 7.0). Purification of TonB-CTD is as described previously (Peacock *et al.* 2005). Isotope labeling and purification of FecA-N terminal domain was also done as previously described (Garcia Herrero & Vogel 2005).

Fluorescence

Gallium enterobactin (1.5 mM) in a 20% (vol/vol) methanol was titrated into 10 μM FepA cork domain in 10 mM Sodium Phosphate buffer pH 7.0, 5% MeOH (vol/vol) in a Varian Cary Eclipse fluorimeter. Excitation was at 295 nm with the excitation slit width at 5 nm. The emission spectra were measured from 310 nm to 450 nm with an excitation slit width of 5 nm. The maximum emission intensity was found to be at 351 nm and

quenching due to the gallium enterobactin was fit to a rectangular hyperbola to determine the dissociation constant using the Grace software package (http://plasma-gate.weizmann.ac.il/Grace/).

Circular dichroism

Circular Dichroism experiments were performed on a Jasco J-715 Spectropolarimeter using the following parameters: wavelength downscan from 260 to 180 nm, step resolution of 0.1 nm, speed of 50 nm/min, 3 accumulations, 1 s response time, 20 mdeg sensitivity, and a band width of 5 nm. Samples of 50 μM FepA cork domain were measured in the presence and absence of 50 μM ferric-enterobactin.

Fourier transform infrared spectroscopy

All FTIR absorption spectra were collected with an Equinox 55 FTIR spectrophotometer (Bruker Optics, Billerica, MA) with a demountable transmission cell consisting of two BaF_2 windows. The special design of the bottom window (Kalnin & Venyaminov 1987) provided a pathlength of 50 μm without the need to use a spacer.

A total of 256 scans were accumulated for each spectrum at 4 cm^{-1} resolution using a deuterated tryglycine sulfate (DTGS) detector. Water vapour traces were removed using the Atmospheric Water Compensation subroutine in the Opus 4.2 (Bruker Optics) software. Solvent spectra obtained under the same conditions were subtracted from all sample spectra. Baseline correction was performed by the Opus 4.2 software. IR absorption spectra used for band fitting were normalized to 2.0 a.u. (absorption units).

Samples measured included 125 μM FepA Cork domain with and without 125 μM ^{13}C labeled TonB-CTD, as well as in the presence and absence of ferric-enterobactin. All measurements were done in a 10 mM sodium phosphate buffer pH 7 containing 5% (vol/vol) methanol. Also measured was 125 μM ^{13}C and unlabelled TonB-CTD in 10 mM sodium phosphate pH 7 buffer with and without 5% methanol, as well as with 125 μM FecA N-terminal domain.

All spectral manipulations (subtractions, additions, etc.) were performed using the Opus 4.2 software. Due to overlap of the amide I' band of ^{13}C-labeled TonB-CTD with the side chain bands of the other protein in the mixture it was not possible to directly compare the spectra of the mixtures with the spectra of the individual proteins. Subtraction of the previously published side chain contributions from all spectra would facilitate this task, however in addition to the assumption that there are no changes in the interaction between the protein side chains, spectral artifacts are highly probable in such a procedure due to differences in the experimental in the current study and in the previously obtained spectra of various protein side chains (Chirgadze *et al*. 1975). Therefore, we produced the calculated spectra of the mixtures by adding the experimental spectra of the corresponding individual proteins. Due to the 1:1 molar ratio of the component proteins in the mixtures, no scaling was required. Comparing such calculated spectra of the mixtures with the experimental spectra allowed accounting for the overlap of the amide I' band of ^{13}C labeled TonB with the side chain bands of the other protein in the mixture.

The calculated spectra were considered to represent the spectra of the mixtures with no protein interaction. Therefore, differences between the calculated spectra and the actual measured spectra of the mixtures would arise due to the protein–protein interaction. Nevertheless, we still made the assumption that the main contribution to these spectral differences would come from the changes in the protein secondary structure and less so from the side chain interactions.

Second derivative spectra were obtained with the Opus 4.2 software with prior 5-point Savitzky-Golay smoothing of the original spectra. The least square curve fitting of the spectra was performed in Origin 7.0 (OriginLab Corporation, Northampton, MA) using the advanced peak fitting module. Initial positions of the individual bands were determined from the second derivative spectra. A Voigt bandshape was used for the component bands. The area under each component band was calculated and considered to represent the amount of a certain type of secondary structure.

NMR

^{1}H,^{15}N HSQC and steady state NOE spectra were acquired on either a Bruker AVANCE 500 MHz spectrometer with a triple resonance inverse cryo-

probe with a single-axis *z*-gradient or a Bruker AVANCE 700 MHz spectrometer equipped with a TXI probe (700 MHz) with a single-axis *z*-gradient. HSQC spectra were typically acquired at 25 °C with 2048 and 256 complex points in the ^{1}H and ^{15}N dimensions with spectral widths of 14 and 35 ppm, respectively. Data was then apodized using a shifted sine bell function, and zero filled prior to Fourier transform using the NMRPipe software package (Delaglio *et al*. 1995). The data was then analyzed in NMRView (Johnson & Blevins 1994). Proton chemical shifts were referenced to 2,2-dimethyl-2-silapentane-5-sulfonate (DSS) as 0 ppm and ^{15}N chemical shifts were referenced indirectly to DSS.

Ferric-enterobactin and iron free enterobactin were purchased from Biophore Research Products. Gallium-enterobactin was made by dissolving iron-free enterobactin in $GaNO_3$ in 5% MeOH solution.

Solutions used for HSQC analysis included: 200 μM ^{15}N TonB-CTD in the presence and absence of 200 μM FepA cork domain, 200 μM FepA cork domain and 400 μM gallium enterobactin, 400 μM gallium, and 200 μM unlabelled FecA N-terminal domain; 200 μM ^{15}N FepA cork domain in the presence and absence of 400 μM gallium-enterobactin, 400 μM gallium-enterobactin and 200 μM unlabelled TonB-CTD, and 200 μM unlabelled TonB-CTD; 200 μM ^{15}N FecA N-terminal domain in the presence and absence of 200 μM unlabelled TonB-CTD.

Results

FTIR

Isotope-edited FTIR spectroscopy provides a convenient method to study protein–protein and protein–peptide interactions. By totally labeling one of the proteins with ^{13}C, its amide I' peak (representing backbone carbonyl stretch vibrations) shifts by $\sim$50 cm^{-1}, allowing analysis of the peaks from the two proteins separately (Haris *et al*. 1992; Zhang *et al*. 1994; Fabian & Vogel 2002). TonB-CTD spectra (unlabelled) display two major peaks between 1630 and 1642 cm^{-1} (not shown), suggesting major contributions from β-sheet conformation with some unordered structures (Byler & Susi 1986; Surewicz & Mantsch 1988; Jackson & Mantsch, 1995; Haris & Chapman 1995; Fabian *et al*. 1996; Fabian & Vogel 2002), consistent with the previously determined solution structure of TonB-CTD. Therefore the band maximum appearing in the spectrum of ^{13}C labeled TonB-CTD around 1593 cm^{-1} can be considered to represent this structure (Figure 4a). Shifts to higher wavenumbers in the experimental spectra compared to those appearing in the calculated spectra indicates an increase in random coil structure, while a shift to lower wavenumbers represents a strengthening of hydrogen bonding in β-sheet conformations.

The band at 1641 cm^{-1} in the FepA cork domain indicates that this protein is primarily composed of random coil structure (Figure 4a) (Byler & Susi 1986; Surewicz & Mantsch 1988; Jackson & Mantsch 1995; Haris & Chapman 1995; Fabian *et al*. 1996; Fabian & Vogel 2002). The shoulder around 1666 cm^{-1} might indicate the presence of some turn structures in the FepA cork domain. The band at 1580 cm^{-1} in the FepA cork domain arises from the protein side chain absorptions (Chirgadze *et al*. 1975; Goormaghtigh *et al*. 1994; Barth 2000).

Addition of ferric-enterobactin resulted in minor changes in the IR spectrum of the FepA cork domain. Band fitting calculations estimated a slight increase in β-sheet structure on the order of 5% with a concomitant decrease in random coil structure (data not shown).

The spectrum of the mixture of the FepA cork domain and TonB-CTD represents a combination of the spectra from both proteins (Figure 4a). The band at 1599 cm^{-1} appears due to overlap of the FepA cork domain side chain band and the TonB-CTD amide I' band. The relatively large high-wavenumber shift of this band from 1589 cm^{-1} in the calculated spectrum to 1599 cm^{-1} in the experimental spectrum suggests a decrease in the amount of β-sheet structure in TonB-CTD. As second derivative and band fitting suggests, this band consists of two main components, at 1604 cm^{-1} and 1584–1588 cm^{-1} (Figure 4b–d). Comparison of the absolute areas of these two components in the calculated and experimental spectrum shows that while they have comparable areas in the calculated spectrum, the area of the high-wavenumber band becomes noticeably larger than the area of the low-wavenumber band in the experimental spectrum. Such integral intensity redistribution appears in the measured spectrum as

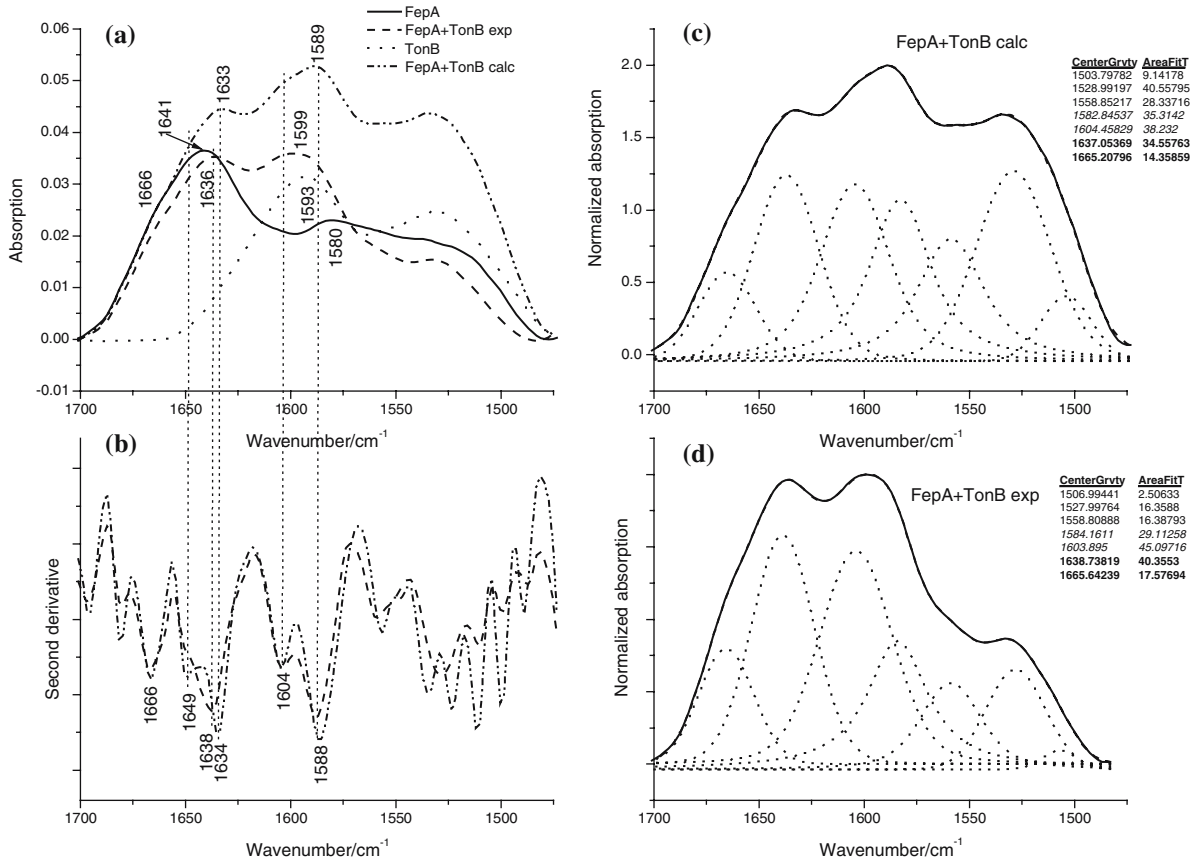

Figure 4. Experimental IR spectra of FepA, TonB, FepA-TonB complex, and calculated spectrum of FepA + TonB (a); second derivative spectra of experimental IR spectrum of FepA–TonB complex and calculated spectrum of FepA + TonB (b); results of the least squares band fitting of the calculated spectrum of FepA + TonB (c) and experimental spectrum of FepA–TonB complex (d). Center of gravity and area under the curve is given for component bands. Values for peaks assigned to TonB are in italic, values for peaks assigned to FepA are in bold.

a shift from 1589 to 1599 cm^{-1}. Suggesting that the low-wavenumber band represents contributions from the β-sheet structures and the high-wavenumber band represents contributions form the random coil fragments, the spectral changes show a slight decrease in the β-sheet conformation of TonB-CTD upon interaction with the FepA cork domain.

The IR band at 1636 cm^{-1} and the shoulder at 1666 cm^{-1} in the experimental spectrum of the FepA cork domain and TonB-CTD mixture might indicate the presence of β-turn structures in FepA cork domain with the band at 1666 cm^{-1} coming from the loop regions of the turns and the band at 1636 cm^{-1} arising from supporting H-bonds in the turns (Surewicz & Mantsch 1988; Mantsch *et al.* 1993; Hollosi *et al.* 1994). Alternatively (but less likely), the low-wavenumber band might be assigned to very strongly H-bonded random coil fragments. The low-wavenumber band appears in the calculated spectrum at 1634–1637 cm^{-1} according to the second derivative and band fitting. However, in the experimental spectrum it is slightly shifted to 1638–1639 cm^{-1}, indicating very minor weakening in the H-bonding in the FepA cork domain upon interaction with TonB-CTD. This could happen either due to weakening of the supporting H-bonds in the turns or due to weaker or less extensive H-bonding with water molecules, possibly due to lower water accessibility of the FepA cork domain regions upon interaction with TonB-CTD.

The amide I' band maximum of TonB-CTD in the calculated spectrum of the FecA–TonB mixture appears at 1588 cm^{-1}, while it shifts to 1594 cm^{-1} in the experimental spectrum indicating

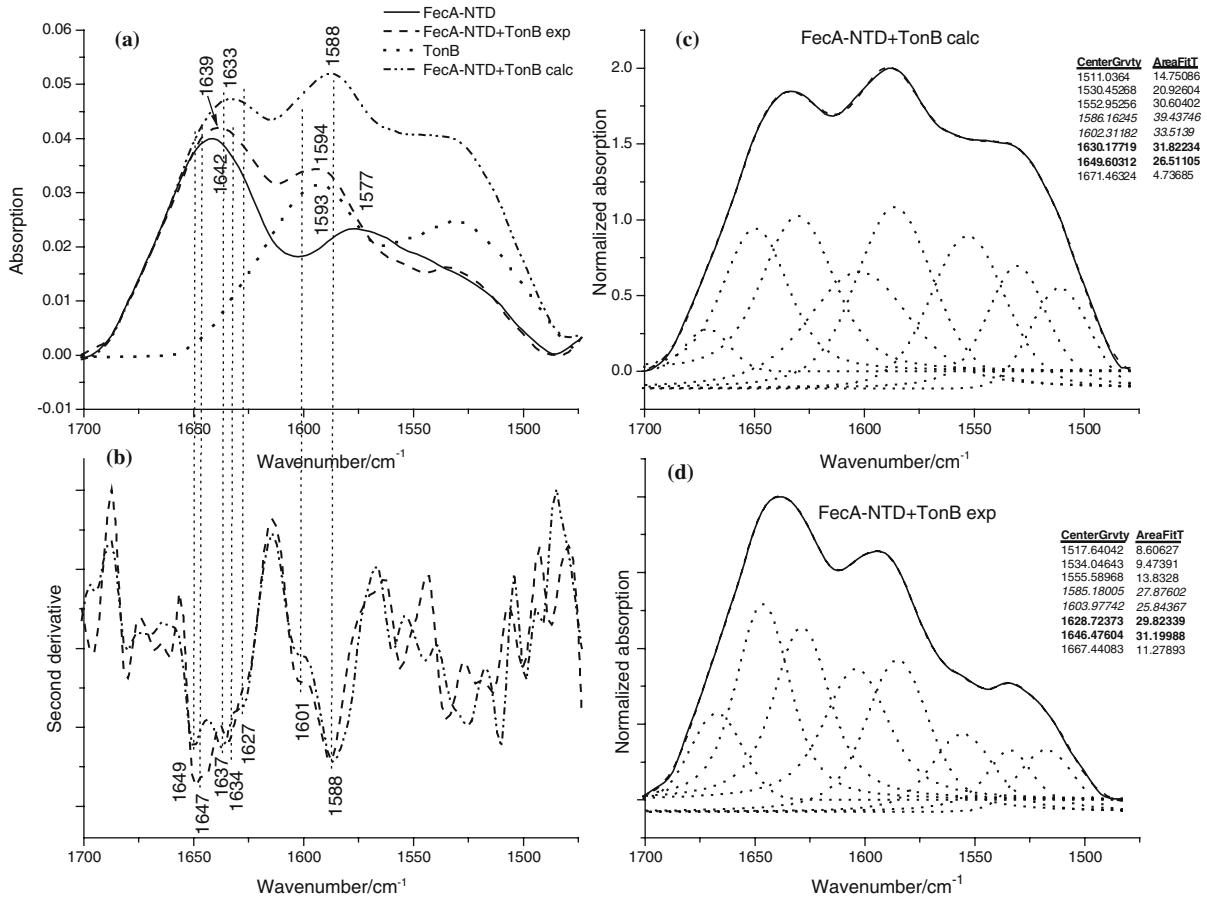

Figure 5. Experimental IR spectra of FecA–NTD, TonB, FecA–NTD–TonB complex, and calculated spectrum of FecA–NTD + TonB (a); second derivative spectra of experimental IR spectrum of FecA–NTD–TonB complex and calculated spectrum of FecA–NTD + TonB (b); results of the least squares band fitting of the calculated spectrum of FecA–NTD + TonB (c) and experimental spectrum of FecA–NTD–TonB complex (d). Center of gravity and area under the curve is given for component bands. Values for peaks assigned to TonB are in italic, values for peaks assigned to FecA–NTD are in bold.

a decrease in the β-sheet and an increase in random coil structure in TonB-CTD (Figure 5a). Two major components, comprising this band, as revealed by the second derivative and band fitting, appear at 1585–1588 and 1601–1604 cm^{-1}. Band fitting demonstrates that the low-wavenumber component has a slightly larger area than the high-wavenumber component in the calculated spectrum, while they appear almost equal in the experimental spectrum. In this case the band area redistribution brings about the apparent band maximum shift in the experimental spectrum from 1588 to 1594 cm^{-1}, and it also suggests a slight decrease in the β-sheet structure and an increase in the random coil structure of TonB.

The FecA N-terminal domain amide I' band in the calculated spectrum of FecA–TonB mixture is centered at 1633 cm^{-1} and, according to the second derivative and band fitting, is composed of two major components, representing contributions from random coil and β-sheet structures at 1649 and ~1630 cm^{-1}, respectively (Figure 5b–d) (Byler & Susi 1986; Surewicz & Mantsch 1988; Jackson & Mantsch 1995; Haris & Chapman 1995; Fabian *et al*. 1996; Fabian & Vogel 2002). These two components are retained in the experimental spectrum as well. However, the band fitting shows that while the area of the β-sheet component is slightly larger in the calculated spectrum, it is equal or slightly smaller in the experimental spectrum. Such integral intensity redistribution is apparent as a shift of the FecA N-terminal domain composite band maximum from 1633 cm^{-1} in the calculated to 1639 cm^{-1} in the experimentally

measured spectrum of the FecA–TonB mixture. These spectral changes indicate a slight decrease in the β-sheet structure of FecA N-terminal domain and some increase of the random coil elements upon interaction with TonB.

Circular dichroism

In order to verify the FTIR data, we examined the CD spectra of the FepA cork domain in the presence and absence of ferric-enterobactin. The results were similar to those obtained by FTIR. The FepA cork domain gave a CD spectrum that was representative of a mostly random coil protein, with the addition of ferric-enterobactin resulting in essentially no change in the spectrum (Figure 6).

NMR spectroscopy

The $^{1}H-^{15}N$ HSQC spectra of the FepA cork domain was much as described for the *E. coli* FepA cork domain. Essentially all of the correlations are within the chemical shift range 7.5–8.5 ppm, which is indicative of a total random coil structure (Figure 7). The steady state NOE spectrum of the FepA Cork domain revealed that all of the visible correlations have negative NOEs, further demonstrating that the FepA cork domain in the absence of the barrel is almost completely unstructured on the NMR time scale.

When gallium enterobactin was added to the FepA cork domain, several small areas of the highly overlapped HSQC spectrum were broadened, but no new distinct upfield or downfield correlations were seen to appear that would characterize the formation of secondary structure. Addition of gallium enterobactin in a 20% methanol solution which helps to solubilize the enterobactin resulted in the sharpening and downfield shifting of a number of peaks in the HSQC, but is essentially identical to the HSQC of FepA cork domain in 20% methanol in the absence of any gallium enterobactin.

Addition of unlabelled TonB-CTD caused several peaks to broaden beyond detection, however no very distinct new correlations are observed either upfield or downfield of the characteristic random coil chemical shift region (Figure 7). Further addition of gallium enterobactin had no noticeable effects on the HSQC spectra.

When unlabelled FepA cork domain was added to TonB-CTD however, many changes were

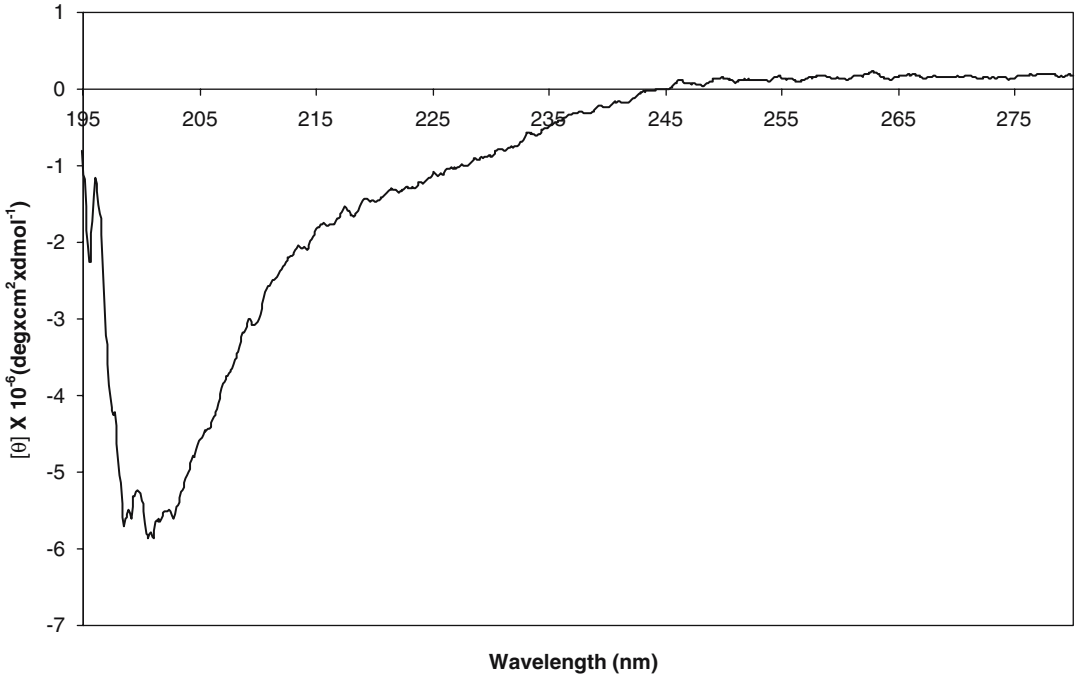

Figure 6. CD spectrum of the FepA cork domain.

observed in the TonB-CTD HSQC spectrum (Figure 8). Essentially all of the chemical shift changes that are observed when adding 10mer TonB box peptides from FepA or FhuA as described previously (Peacock *et al*. 2005) are seen in the presence of the FepA cork domain. Also of note is an intensifying of highly overlapped peaks in the unfolded region of the spectrum. The reason for this is at this point unclear to us. No new peaks are observed in the structured regions other than those seen previously when adding the TonB box peptides however, indicating that the rest of the FepA cork domain is not inducing any new structure in TonB-CTD.

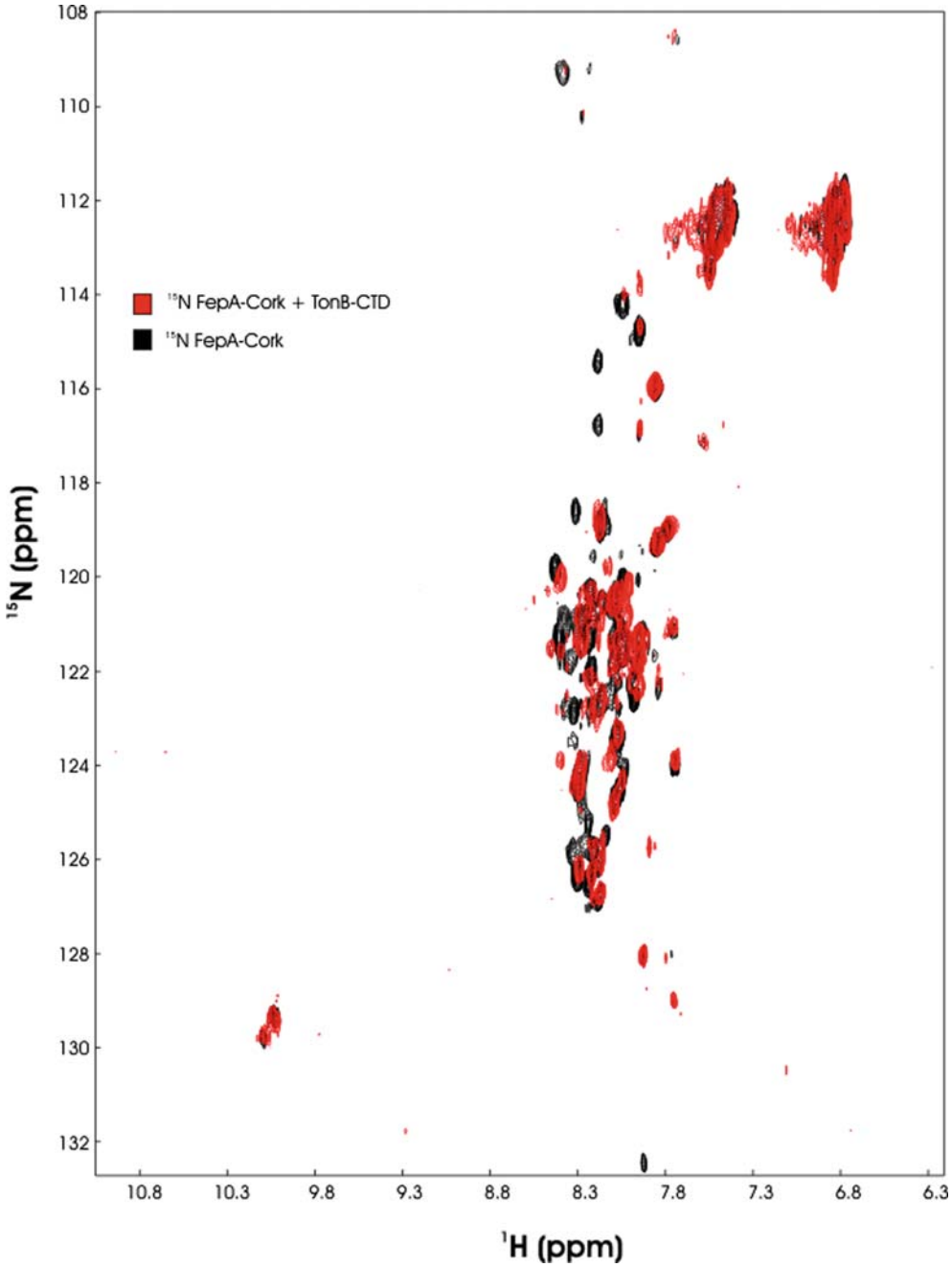

Figure 7. NMR HSQC spectrum of ^{15}N FepA-Cork with TonB-CTD. ^{15}N FepA-Cork is in black, and ^{15}N FepA-Cork with an equimolar amount of TonB-CTD is in red. The spectra are similar except for a broadening/disappearance of several correlations.

Similar experiments were done with the FecA N-terminal domain. Addition of unlabelled FecA N-terminal domain to TonB-CTD failed to elicit any changes in the TonB spectrum, despite the fact that this construct includes the TonB box (data not shown). In the reciprocal experiment, addition of unlabelled TonB-CTD to ^{15}N labeled FecA–NTD resulted in only minor shifts in the HSQC, none of which involved the TonB box residues (Figure 9).

Discussion

The results we obtained with the FepA cork domain from *S. typhimurium* are very similar to those

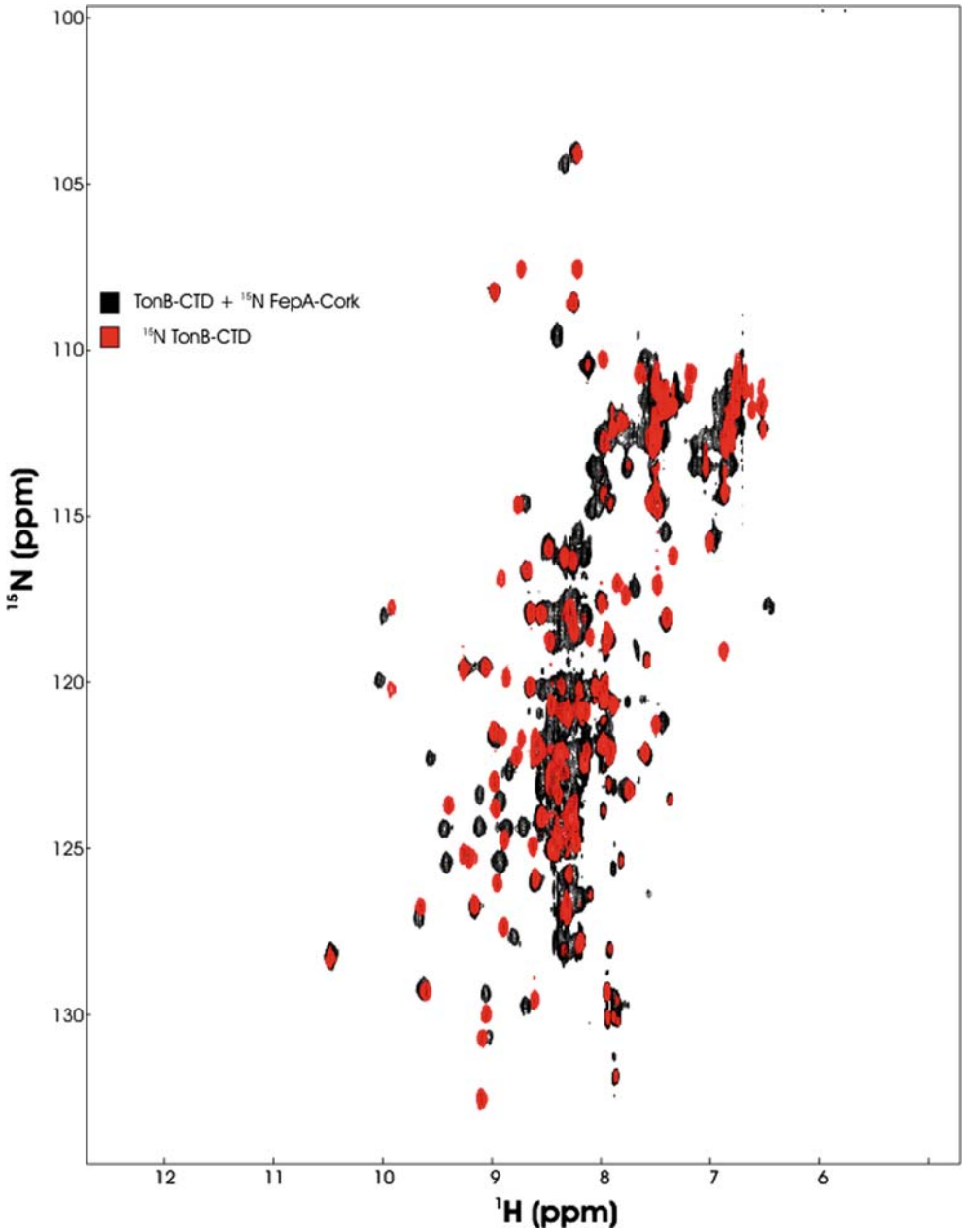

Figure 8. NMR HSQC spectrum of ^{15}N TonB-CTD with FepA-Cork. ^{15}N TonB-CTD is in red, and ^{15}N TonB-CTD with FepA-Cork is in black. Many correlations shift in ^{15}N TonB-CTD, correlating exactly with the changes seen when adding only FepA TonB-Box peptide.

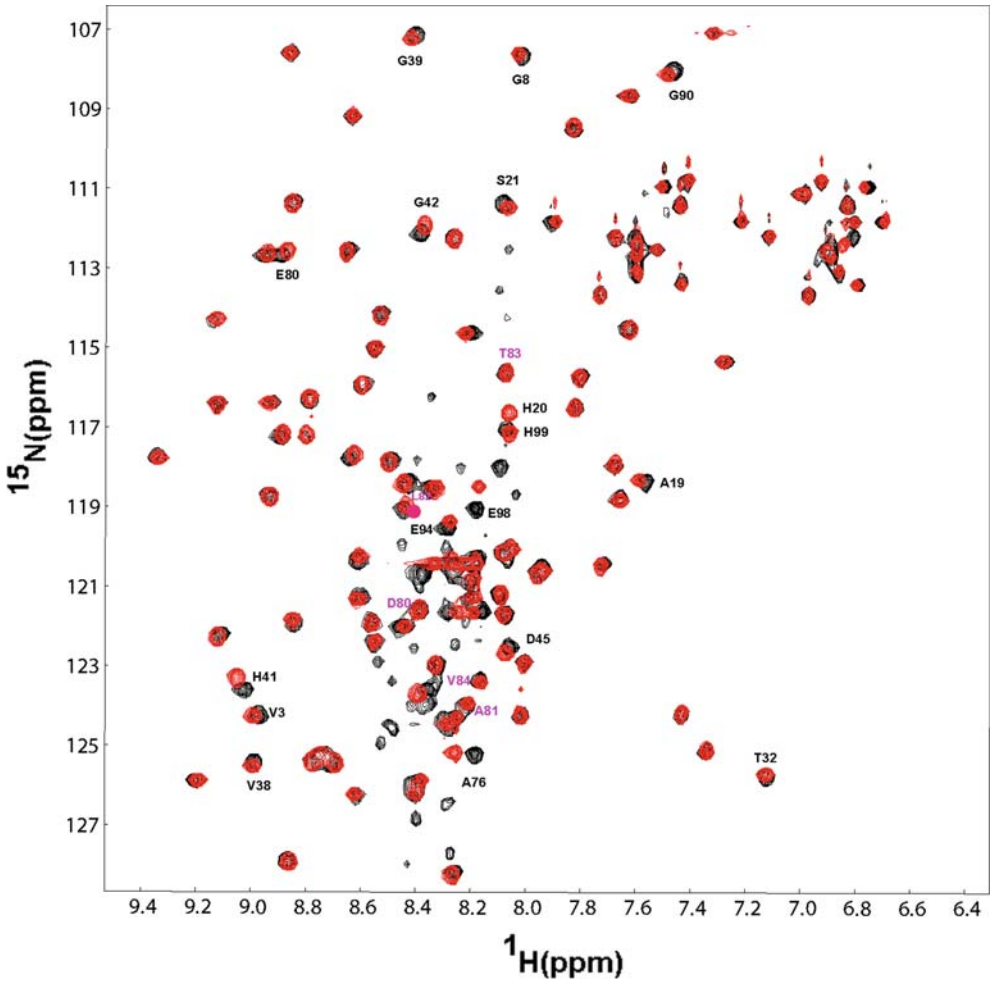

Figure 9. HSQC spectrum of ^{15}N FecA–NTD with TonB-CTD. Only a few correlations shift very slightly, and the peaks associated with the TonB box residues (highlighted in purple) are unaffected.

obtained using the *E. coli* FepA cork domain (Usher *et al.* 2001) as both these constructs were found to be essentially unstructured in solution. The *E. coli* construct did show several weak amide peaks detected by NMR in the region characteristic of β-sheet, but these may have to do with sequence differences between the *E. coli* and *Salmonella* cork domains, or differences in the preparation. Overall these results showed that very few, if any structural changes resulted upon the binding of the siderophore to the cork domain that could be observed by NMR. Usher *et al.* also measured the binding of gallium enterobactin to the FepA Cork domain by measuring the fluorescence anisotropy of the enterobactin. We also determined the binding constant by measuring the quenching ofthe tryptophan in the *Salmonella* FepA cork domain by gallium enterobactin, using the quenching of an aqueous solution of tryptophan as a control. Although the tryptophan would not be predicted to be close to the gallium enterobactin if one were to assume that (a) the structure in solution was the same as in the barrel and (b) the binding site is close to the apical loops on the extracellular side of the transporter, we did observe quenching which yielded a binding constant of $\pm 2\mu$M, which is very similar to the value reported for the *E. coli* FepA cork domain. Attempts to characterize the binding by isothermal titration calorimetry failed due to difficulties in matching the MeOH concentrations between the titrant with the Ga-enterobactin and the protein in the cell chamber. Futhermore,

differential scanning calorimetry trials failed to give any transitions in either the ligand-free or ligand-bound states. This was probably due to the inherent disorder of the isolated cork domain. Attempts to characterize the binding of TonB-CTD to the cork domain by tryptophan fluorescence were not undertaken as previous studies with TonB box peptides had shown that the environment of the single tryptophan in TonB-CTD was unaffected by the binding of the peptides (data not shown).

The results from the FTIR studies confirmed those obtained by NMR. No large amount of structure appears to be conferred on the FepA cork domain by TonB-CTD, and TonB-CTD appears to become somewhat disordered in the presence of FepA. This is consistent with our observation that the C-terminal β-strand of TonB-CTD observed in the solution structure becomes disordered upon binding of TonB box peptides (unpublished observations). This appears to be an unusual phenomenon, as it is more common in the literature to see reports of unstructured polypeptides gaining more order upon binding to a partner (Dyson & Wright 2005). However, it is possible that this increased disorder could increase the surface area of TonB to bind to other parts of the OMT, or other proteins, for example in a homodimerization event as reported in other studies (Chang *et al.* 2001; Khursigara *et al.* 2004; Khursigara *et al.* 2005; Koedding *et al.* 2005). Nonetheless, these results must be interpreted cautiously due to the fact that it is unclear as to whether the cork domain would ever be in contact with TonB in this state.

We were very surprised to discover that the FecA N-terminal domain did not appear to interact with TonB-CTD in the same way as the FepA cork domain. Both contain the TonB box, and in both cases the TonB box is apparently completely mobile and presumably accessible. It could be that the structure of the FecA N-terminal domain is in some way inhibiting the binding of TonB-CTD to the TonB box so even though the sequence itself is sufficient to promote binding to TonB-CTD, the context of the TonB box can either inhibit or promote binding. Alternatively, there is a histidine tag at the extreme C-terminus of the FecA N-terminal domain construct which may in some way interfere with TonB-CTD binding.

The answer as to the state of the cork domain during siderophore transport remains an elusive problem. In our study we have discovered subtle structural changes in TonB-CTD when bound to the isolated cork domain of FepA. Moreover we observed that there may be additional impediments to binding of TonB to OMT_N imposed by the N-terminal signaling domain of FecA. If the cork is indeed partially or fully ejected into the periplasmic space, then this interaction may well be relevant *in vivo*. Future studies of TonB bound to intact receptors will hopefully give us additional clues as to how TonB promotes siderophore transport into the periplasmic space.

Acknowledgements

This work was supported by an operating grant from the Canadian Institutes for Health Research (CIHR) to H.J.V.. R.S.P. was supported by Studentship awards from the Alberta Heritage Foundation for Medical Research (AHFMR) and the National Science and Engineering Research Council (NSERC). A.G.H. is supported by a Postdoctoral Fellowship award from the Alberta Ingenuity Fund. HJV holds a Scientist award from AHFMR. The NMR equipment used was obtained through grants from the Canada Foundation for Innovation, the Alberta Science and Research Authority (ASRA) and AHFMR. Maintenance of the Bio-NMR centre is supported by CIHR and the University of Calgary. The FTIR equipment was funded by the Alberta Network for Proteomics Innovation which was funded in turn by the Western Economic Diversification program, and ASRA.

References

Aiyar A. 2000 The use of CLUSTAL W and CLUSTAL X for multiple sequence alignment. *Methods Mol Biol* **132**, 221–241.

Barth A. 2000 The infrared absorption of amino acid side chains. *Prog Biophys Mol Biol* **74**, 141–173.

Bonhivers M, Desmadril M, Moeck GS, *et al.* 2001 Stability studies of FhuA, a two-domain outer membrane from *Escherichia Coli*. *Biochemistry* **40**, 2606–2613.

Braun V. 2003 Iron uptake by *Escherichia coli*. *Front Biosci* **8**, s1409–s1421.

Braun V, Mahren S. 2005 Transmembrane transcriptional control (surface signalling) of the Escherichia coli Fec type. *FEMS Microbiol Rev* **29**, 673–684.

Buchanan SK, Smith BS, Venkatramani L, *et al.* 1999 Crystal structure of the outer membrane active transporter FepA from *Escherichia coli*. *Nat Struct Biol* **6**, 56–63.

Byler DM, Susi H. 1986 Examination of the secondary structure of proteins by deconvolved FTIR spectra. *Biopolymers* **25**, 469–487.

Chang C, Mooser A, Pluckthun A, Wlodawer A. 2001 Crystal structure of the dimeric C-terminal domain of TonB reveals a novel fold. *J Biol Chem* **276**, 27535–27540.

Chimento DP, Kadner RJ, Wiener MC. 2005 Comparative structural analysis of TonB-dependent outer membrane transporters: implications for the transport cycle. *Proteins* **59**, 240–251.

Chirgadze YN, Fedorov OV, Trushina NP. 1975 Estimation of amino acid residue side-chain absorption in the infrared spectra of protein solutions in heavy water. *Biopolymers* **14**, 679–694.

Cobessi D, Celia H, Folschweiller N, *et al*. 2005a The crystal structure of the pyoverdine outer membrane receptor FpvA from Pseudomonas aeruginosa at 3.6 angstroms resolution. *J Mol Biol* **347**, 121–134.

Cobessi D, Celia H, Pattus F. 2005b Crystal structure at high resolution of ferric-pyochelin and its membrane receptor FptA from Pseudomonas aeruginosa. *J Mol Biol* **352**, 893–904.

Delaglio F, Grzesiek S, Vuister GW, *et al*. 1995 NMRPipe: a multidimensional spectral processing system based on UNIX pipes. *J Biomol NMR* **6**, 277–293.

Dyson HJ, Wright PE. 2005 Intrinsically unstructured proteins and their functions. *Nat Rev Mol Cell Biol* **6**, 197–208.

Eisenhauer HA, Shames S, Pawelek PD, Coulton JW. 2005 Siderophore transport through Escherichia coli outer membrane receptor FhuA with disulfide-tethered cork and barrel domains. *J Biol Chem* **280**, 30574–30580.

Fabian H, Vogel HJ. 2002 Fourier transform infrared spectroscopy of calcium-binding proteins. *Methods Mol Biol* **173**, 57–74.

Fabian H, Yuan T, Vogel HJ, Mantsch HH. 1996 Comparative analysis of the amino- and carboxy-terminal domains of calmodulin by Fourier transform infrared spectroscopy. *Eur Biophys J* **24**, 195–201.

Faraldo-Gomez JD, Smith GR, Sansom MS. 2003 Molecular dynamics simulations of the bacterial outer membrane protein FhuA: a comparative study of the ferrichrome-free and bound states. *Biophys J* **85**, 1406–1420.

Ferguson AD, Braun V, Fiedler HP, *et al*. 2000 Crystal structure of the antibiotic albomycin in complex with the outer membrane transporter FhuA. *Protein Sci* **9**, 956–963.

Ferguson AD, Chakraborty R, Smith BS, *et al*. 2002 Structural basis of gating by the outer membrane transporter FecA. *Science* **295**, 1715–1719.

Ferguson AD, Hofmann E, Coulton JW, Diederichs K, Welte W. 1998 Siderophore-mediated iron transport: crystal structure of FhuA with bound lipopolysaccharide. *Science* **282**, 2215–2220.

Garcia Herrero A, Vogel HJ. 2005 Nuclear magnetic resonance solution structure of the periplasmic signalling domain of the TonB-dependent outer membrane transporter FecA from *Escherichia coli*. *Mol Microbiol* **58**, 1226–1237.

Goormaghtigh E, Cabiaux V, Ruysschaert JM. 1994 Determination of soluble and membrane protein structure by Fourier transform infrared spectroscopy. III. Secondary structures. *Subcell Biochem* **23**, 405–450.

Guex N 2001 DeepView – The Swiss-PDBViewer User Guide.

Haris PI, Chapman D. 1995 The conformational analysis of peptides using Fourier transform IR spectroscopy. *Biopolymers* **37**, 251–263.

Haris PI, Robillard GT, Van Dijk AA, Chapman D. 1992 Potential of 13C and 15N labeling for studying protein-protein interactions using Fourier transform infrared spectroscopy. *Biochemistry* **31**, 6279–6284.

Hollosi M, Majer Z, Ronai AZ, *et al*. 1994 CD and Fourier transform ir spectroscopic studies of peptides. II. Detection of beta-turns in linear peptides. *Biopolymers* **34**, 177–185.

Jackson M, Mantsch HH. 1995 The use and misuse of FTIR spectroscopy in the determination of protein structure. *Crit Rev Biochem Mol Biol* **30**, 95–120.

Johnson BA, Blevins RA. 1994 NMRView – A computer program for the visualization and analysis of NMR data. *J Biomol NMR* **4**, 603–614.

Kalnin N, Venyaminov S. 1987 Quantitative measurements of water solution IR spectra. *J Appl Spectrosc* **4**, 592–597.

Khursigara CM, De Crescenzo G, Pawelek PD, Coulton JW. 2004 Enhanced binding of TonB to a ligand-loaded outer membrane receptor: Role of the oligomeric state of TonB in formation of a functional FhuA-TonB complex. *J Biol Chem* **279**, 7405–7412.

Khursigara CM, De Crescenzo G, Pawelek PD, Coulton JW. 2005 Deletion of the proline-rich region of TonB disrupts formation of a 2:1 complex with FhuA, an outer membrane receptor of Escherichia coli. *Protein Sci* **14**, 1266–1273.

Klebba PE. 2003 Three paradoxes of ferric enterobactin uptake. *Front Biosci* **8**, s1422–s1436.

Koebnik R. 2005 TonB-dependent trans-envelope signalling: the exception or the rule?. *Trends Microbiol* **13**, 343–347.

Koedding J, Killig F, Polzer P, *et al*. 2005 Crystal structure of a 92-residue C-terminal fragment of TonB from Escherichia coli reveals significant conformational changes compared to structures of smaller TonB fragments. *J Biol Chem* **280**, 3022–3028.

Kurisu G, Zakharov SD, Zhalnina MV, *et al*. 2003 The structure of BtuB with bound colicin E3 R-domain implies a translocon. *Nat Struct Biol* **10**, 948–954.

Letoffe S, Wecker K, Delepierre M, Delepelaire P, Wandersman C. 2005 Activities of the Serratia marcescens heme receptor HasR and isolated plug and beta-barrel domains: the beta-barrel forms a heme-specific channel. *J Bacteriol* **187**, 4637–4645.

Mantsch HH, Perczel A, Hollosi M, Fasman GD. 1993 Characterization of beta-turns in cyclic hexapeptides in solution by Fourier transform IR spectroscopy. *Biopolymers* **33**, 201–207.

Oke M, Sarra R, Ghirlando R, *et al*. 2004 The plug domain of a neisserial TonB-dependent transporter retains structural integrity in the absence of its transmembrane beta-barrel. *FEBS Lett* **564**, 294–300.

Peacock RS, Weljie AM, Howard S.P., Price FD, Vogel HJ. 2005 The solution structure of the C-terminal domain of TonB and interaction studies with TonB box peptides. *J Mol Biol* **345**, 1185–1197.

Postle K, Kadner RJ. 2003 Touch and go: tying TonB to transport. *Mol Microbiol* **49**, 869–882.

Ratledge C, Dover LG. 2000 Iron metabolism in pathogenic bacteria. *Annu Rev Microbiol* **54**, 881–941.

Schalk IJ, Yue WW, Buchanan SK. 2004 Recognition of iron-free siderophores by TonB-dependent iron transporters. *Mol Microbiol* **54**, 14–22.

Surewicz WK, Mantsch HH. 1988 New insight into protein secondary structure from resolution-enhanced infrared spectra. *Biochim Biophys Acta* **952**, 115–130.

Usher KC, Ozkan E, Gardner KH, Deisenhofer J. 2001 The plug domain of FepA, a TonB-dependent transport protein from Escherichia coli, binds its siderophore in the absence of the transmembrane barrel domain. *Proc Natl Acad Sci USA* **98**, 10676–10681.

Wiener MC. 2005 TonB-dependent outer membrane transport: going for Baroque?. *Curr Opin Struct Biol* **15**, 394–400.

Yue WW, Grizot S, Buchanan SK. 2003 Structural evidence for iron-free citrate and ferric citrate binding to the TonB-dependent outer membrane transporter FecA. *J Mol Biol* **332**, 353–368.

Zhang M, Fabian H, Mantsch HH, Vogel HJ. 1994 Isotope-edited Fourier transform infrared spectroscopy studies of calmodulin's interaction with its target peptides. *Biochemistry* **33**, 10883–10888.